Colloids and Surfaces A: Physicochem. Eng. Aspects 520 (2017) 736–742

Contents lists available at ScienceDirect

Colloids and Surfaces A: Physicochemical and Engineering Aspects

journal homepage: www.elsevier.com/locate/colsurfa

High hiding power and weather durability of film-coated titanium dioxide particles with a yolk-shell structure

Yong Liang, Keyi Yu, Jiuren Xie, Qinzhong Zheng, Ting-Jie Wang*

Department of Chemical Engineering, Tsinghua University, Beijing 100084, China

HIGHLIGHTS

- TiO_2@void@SiO_2 structure was prepared by surface-protected etching.
- The void in the yolk-shell structure increased the refractive index difference.
- TiO_2@void@SiO_2 has high hiding power and low weather durability.
- TiO_2@MgO@void@SiO_2 was prepared to increase weather durability.
- TiO_2@MgO@void@SiO_2 structure saves TiO_2 consumption 21.2%.

GRAPHICAL ABSTRACT

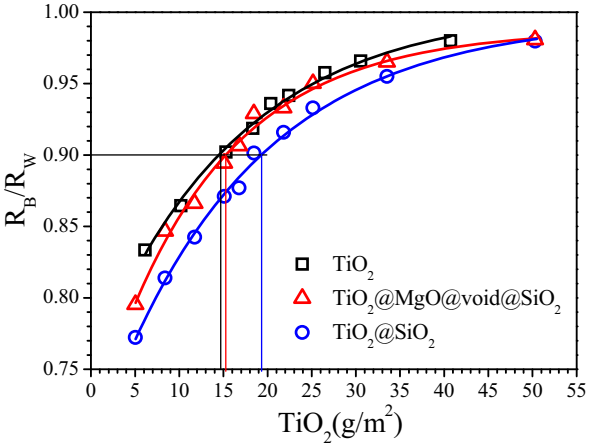

Yolk-shell TiO_2@MgO@void@SiO_2 pigment exhibited high hiding power and weather durability. Compared with the same coating amount of 20% in dense film, the consumption of coated TiO_2 is reduced over 20%.

ARTICLE INFO

Article history:
Received 18 January 2017
Received in revised form 17 February 2017
Accepted 18 February 2017

Keywords:
Titanium dioxide
Coating
Yolk-shell structure
Hiding power
Weather durability

ABSTRACT

High hiding power and weather durability are the key characteristic indices of the high-performance pigmentary titanium dioxide (TiO_2). The film-coated TiO_2 particles with a yolk-shell structure of silica were prepared by surface-protected etching with polyvinyl pyrrolidone. The hiding power of the TiO_2 particles with the yolk-shell structure was 90.6, which is significantly higher than the hiding power of 87.7 for the dense film-coated TiO_2 particles with the same amount of coating (20%). However, the TiO_2 particles with the yolk-shell structure have low weather durability. The apparent degradation rate constant K_{app} for rhodamine-B had a high value of 13.2. An improvement was made by coating a dense MgO film on the TiO_2 particles first, and then coating a yolk-shell structure. The hiding power of the TiO_2 particles with the improved yolk-shell structure reached 90.6, and the weather durability was significantly increased as the apparent degradation rate constant K_{app} decreased to 2.2, reaching the excellent weather durability of the TiO_2 particles with 5 wt% dense film coating (Si3 + Al2), which is a common product in industry (K_{app} = 1.8). For the same indices of hiding power and weather durability, the TiO_2 particles with the improved yolk-shell structure obviously decreased the consumption of TiO_2, compared with the dense SiO_2-coated TiO_2 particles (TiO_2@SiO_2). It is inferred that the void in the yolk-shell structure increased

* Corresponding author.
E-mail address: wangtj@tsinghua.edu.cn (T.-J. Wang).

http://dx.doi.org/10.1016/j.colsurfa.2017.02.046

the light reflectivity of the TiO_2 particles by increasing the difference of the refractive index between the core TiO_2 and the surroundings, and the dense MgO film increased the weather durability of the TiO_2 particles.

1. Introduction

Titanium dioxide (TiO_2) is the best white pigment due to its excellent optical properties, which is widely used in the paints, plastics, paper, ink and other industries. However, TiO_2 particles produce electrons and holes under UV light irradiation and generate radicals after reaction with water and oxygen, resulting in the degradation of the organic matter around the TiO_2 particles [1–4]. Hence, the TiO_2 particles need to be coated with the shield films of inert oxides, e.g., silica and alumina, to increase the weather durability [5–9].

Our previous work has confirmed that as the coating amount of the film-coated TiO_2 particles increased, the apparent degradation rate of rhodamine B by TiO_2 was reduced, i.e., the weather durability of the film-coated TiO_2 particles was increased [10,11]. However, as the coating amount increased, the hiding power of the film-coated TiO_2 particles decreased. The hiding power represents the ability of the TiO_2 particles in a paint layer to cover the background light from the matrix. The higher the hiding power of the TiO_2 particles was, the lower the amount of the TiO_2 was needed, i.e., the lower the cost.

The hiding power of titanium dioxide was not only affected by the particle dispersion in the organic matrix but also by the film refractive index coated on the titanium dioxide particles [12,13]. The hiding power of the film-coated TiO_2 particles was reported to increase as the film refractive index decreases in the range of 1.00–2.15, and the TiO_2 particles with a porous coating film have higher hiding power because the porous film has a lower apparent refractive index [14]. It is inferred that when the refractive index of the film is 1.00 (air), e.g., the yolk-shell structure, the film coated particle of titanium dioxide has the highest hiding power. The polymer yolk-shell structure containing TiO_2 particles in the centers of air void was obtained by using an emulsion polymerization [15]. The yolk-shell structure with air void was found to significantly enhance the pigment reflection in paint films. Compared with the same amount of the same titanium dioxide pigment used conventionally, the hiding power of the yolk-shell structure was increased from 38% to 66% [16]. However, the photocatalytic degradation of Rhodamine-B [17] and methylene blue [18] indicated that yolk-shell coated TiO_2 particles had higher photoactivity, i.e., worse weather durability. It is highly desired to fabricate an improved yolk-shell structure of the coating film on the TiO_2 particle surface to achieve high hiding power and weather durability.

Recently, many strategies for silica coating film with different morphologies on the surface of inorganic nanoparticles have been reported [19], especially for the preparation of a yolk-shell silica structure. Yolk-shell structure has exhibited many unique properties that are not accessible to core shell particles [20,21]. Templating strategies have been widely used for synthesizing yolk-shell structures, for example, the TiO_2/C/SiO_2 sample (core/template/shell) was prepared first, and then the sample was heated at 873 K for 3 h in air to remove carbon components and form the void [22]. This synthetic method is complex and time-consuming. The preparation methods of yolk-shell structures without templates have also been reported, a core shell particle was transformed into a yolk-shell particle directly by selective etching of the core particle [23] and by a surface-protected etching process with polyvinyl pyrrolidone (PVP) [24,25].

In this paper, TiO_2 particles were coated with a yolk-shell structure of silica by surface-protected etching, and the hiding power and weather durability of the coated TiO_2 particles were evaluated. The TiO_2 particles that were first coated with MgO film and then coated with the yolk-shell structure of silica were prepared to achieve high hiding power and high weather durability.

2. Experimental

2.1. Reagents

Commercial TiO_2 particles (technical pure, Jiangsu Hongfeng Titanium Company, China) having the rutile structure and an average diameter of 300 nm were used in the experiments. The TiO_2 particles were produced by the hydrolysis of $TiOSO_4$ and a subsequent calcination. They were pure without any preliminary treatment. All other chemicals used, namely, tetraethylorthosilicate (TEOS), polyvinyl pyrrolidone (PVP, MW ~ 10,000), sodium hydroxide (NaOH), $MgSO_4 \cdot 7H_2O$, ammonium hydroxide ($NH_3 \cdot H_2O$, 28% by weight in water), ethanol, glycerol and rhodamine B, were analytical reagent (AR) grade.

2.2. Coating process

2.2.1. MgO coating on TiO_2 particles (TiO_2@MgO)

150 g TiO_2 particles were mixed with 300 g deionized water by an ultrasonic treatment for 30 min in a three-necked flask. Then $MgSO_4$ solution (1 mol/L) and NaOH solution (4.5 mol/L) were titrated into the TiO_2 suspension separately and simultaneously. The temperature was controlled at 60 °C by a constant temperature bath and the pH of the TiO_2 suspension was kept constant at 5 by adjusting the titration rate of the NaOH solution. After the titration, the suspension was aged for 2 h under stirring. Then, the suspension was filtered and dried at 105 °C for 24 h. The amount of MgO coating was set at 2.0 wt%.

2.2.2. SiO_2 coating on TiO_2 particles (TiO_2@ SiO_2), MgO and SiO_2 double layer coating on TiO_2 particles (TiO_2@MgO@SiO_2)

Ammonium hydroxide solution (10 mL), deionized water (40 mL), ethanol (100 mL) and TiO_2 particles (or TiO_2@MgO particles, 5 g) were mixed in a 250-mL three-neck flask with magnetic stirring. Then, a certain amount of TEOS was titrated into the TiO_2 suspension. The suspension was kept at room temperature under continuous magnetic stirring for 2 h. After aging, the suspension was centrifuged and washed 3 times, and dried at 105 °C for 24 h. The amount of SiO_2 coating was adjusted by controlling the amount of added TEOS.

2.2.3. Surface-protected etching

TiO_2@SiO_2 (5 g) (or TiO_2@MgO@SiO_2 particles) was added and dispersed in 100 mL PVP solution (10 g, MW ~ 10,000) under magnetic stirring. The suspension was heated to 100 °C and kept for 3 h to load PVP on the silica surface, and then cooled to room temperature. Under magnetic stirring, NaOH aqueous solution (30 mL, 0.20 g/mL) was added to the solution to etch the silica

film. After a set time etching, the TiO_2 particles were collected by centrifugation and washed 3 times using deionized water. The samples were marked as TiO_2@void@SiO_2 or TiO_2@MgO@void@SiO_2, respectively.

2.3. Evaluation of the weather durability

The degradation of rhodamine B in the TiO_2 suspension under UV irradiation was used to evaluate the weather durability of the film-coated TiO_2 particles. The photodegradation kinetics of rhodamine-B by TiO_2 particles is a typical heterogeneous catalytic reaction [26–30] and the reaction rate is often approximately described using a first-order kinetic expression when the rhodamine-B concentration is less than 10^{-3} M [31].

The film-coated TiO_2 particles (400 mg) were dispersed in 100 mL of rhodamine-B solution with a concentration of 4 mg/L under magnetic stirring. Air with a flow rate of 50 mL/min was fed into the suspension for keeping the constant oxygen concentration and the temperature was kept at 25 °C. A sufficient dark adsorption was conducted for 30 min before UV irradiation. Then, the suspension was irradiated using UV light from low pressure mercury lamps (dominant wavelength 254 nm, 32 W) for 120 min. At each 30-min interval, the suspension was sampled and centrifuged. The rhodamine-B concentration of the supernatant (C_i, $i = 0, 1, \ldots, 4$) was measured by detecting the characteristic absorbance of rhodamine-B at 554 nm using a UV–vis spectrophotometer (TU-1901Persee, Beijing, China). The $\ln(C/C_0)$ versus t was fitted with a straight line, and the slope is the apparent first-order rate constant, i.e., k_{app} [10,11].

2.4. Evaluation of the light transmittance

The light transmittance of the film-coated TiO_2 particle suspension was examined to confirm the hiding power evaluation. 100 mg of the film-coated TiO_2 particles were dispersed in 100 mL deionized water under an ultrasonic treatment for 30 min to produce TiO_2 suspension at a concentration of 1.0 g/L. For high accuracy, 1 mL of the TiO_2 suspension was taken and diluted to 10 mL using deionized water and then fully dispersed. Then, 1 mL of the diluted TiO_2 suspension was mixed with 1 mL glycerol to form a stable suspension at a concentration of approximately 0.05 g/L. The viscous glycerol allows the TiO_2 particles to be well suspended. The light transmittance of the TiO_2 suspension was measured using a UV–vis spectrophotometer.

2.5. Evaluation of the hiding power

The hiding power of the film-coated TiO_2 particles was measured referring to the literature and standards [14,32]. Firstly, the film-coated TiO_2 particles (12 g) were thoroughly ground in an agate mortar, then the ground TiO_2 particles were mixed with alkyd resin (50.5 g, with density of 900 kg/m^3) completely by using the grinding media of glass beads (100 g) and shaking for 15 min. Secondly, the mixture was painted on the black and white substrates using an automatic coating equipment and the paint layers with different thicknesses were dried for 24 h at room temperature. Thirdly, the reflectivities of the paint layers on the black and white substrates, R_B and R_W, respectively, were measured by a reflectometer. The contrast ratio R_B/R_W change with the amount of TiO_2 per unit area was obtained. In the standard, the contrast ratio R_B/R_W ($\times 100\%$) value is defined as the hiding power of the TiO_2 particles. In this paper, the hiding power for the wet paint layer thickness at 100 μm and the needed amount of TiO_2 per unit area for the hiding power of 90.0 were used for evaluation.

2.6. Characterization

The specific surface area and the pore volume of the film-coated TiO_2 particles were calculated from the Nitrogen adsorption and desorption isotherms at 77 K using a Quantachrome AUTOSORB-1 automated gas sorption instrument (USA). The morphology and structure of the film-coated TiO_2 particles were examined with a high-resolution transmission electron microscope (HRTEM, JEM-2011, JEOL Co., Tokyo, Japan). The coating amounts were determined by X-ray fluorescence spectroscopy (XRF, Shimadzu XRF-1800, Japan).

3. Results and discussion

3.1. TiO_2 particles coated with a yolk-shell structure of silica

A continuous dense SiO_2 film was coated on the surface of the TiO_2 particles with a coating amount of 50 wt% (SiO_2/TiO_2). Then, PVP was loaded on the SiO_2 films, and NaOH solution was added to the suspension to etch the SiO_2 films. The TEM images before and after the etching process are shown in Fig. 1. Fig. 1 shows that the coated film on the TiO_2 particle surface was dense and uniform, with a thickness of approximately 50 nm. After 30 min of etching, the voids appeared at the interface of the core TiO_2 particle and the coated film, and the internal structure of the coated films was porous. After 105 min of etching, obvious void structures formed between the core TiO_2 particle and the film, obtaining the film-coated TiO_2 particles with a yolk-shell structure of silica, marked as TiO_2@void@SiO_2. NaOH was reported to attack the surface silica layer, which is protected by PVP molecules, in the first 30 min of reaction. The initial etching does not completely dissolve the surface layer. Instead, it creates mesoscale pores on the surface so that the etchant can diffuse inside the particles. Due to the PVP protection, the protected silica surface has a slow etching rate [25].

Before etching, the amount coated on the TiO_2 particles was measured to be 48.4% (SiO_2/TiO_2) by XRF (X-ray fluorescence), indicating that almost all the added TEOS was coated on the surface of the TiO_2 particles. After 105 min of etching, the remaining SiO_2 amount on the TiO_2 particle surface was 19.0% (SiO_2/TiO_2). For comparing the yolk-shell structure of the coated films, a dense and continuous SiO_2 film was coated on TiO_2 particles with the coating amount of 20 wt%, which was marked as TiO_2@SiO_2. The nitrogen adsorption and desorption isotherm curves of the yolk-shell struc-

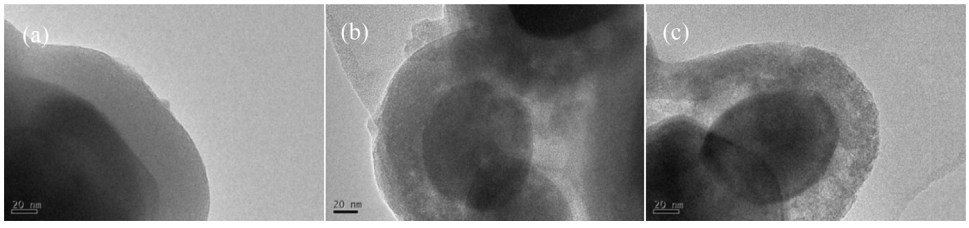

Fig. 1. TEM images of the film-coated TiO_2 particles with different structures: (a) dense film with coating amount 50 wt%(SiO_2/TiO_2); (b) the structure of the film (a) after etching 30 min; (c) the structure of film (a) after etching 105 min.

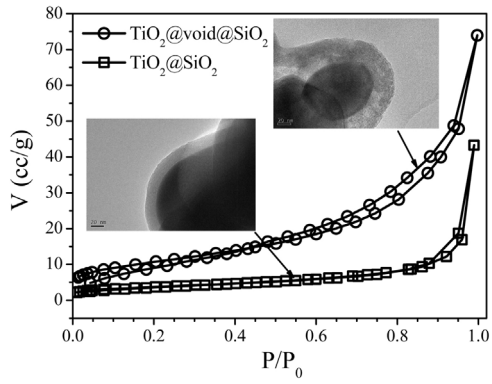

Fig. 2. N_2 adsorption-desorption isotherms of TiO_2@ SiO_2 and TiO_2@void@SiO_2 samples.

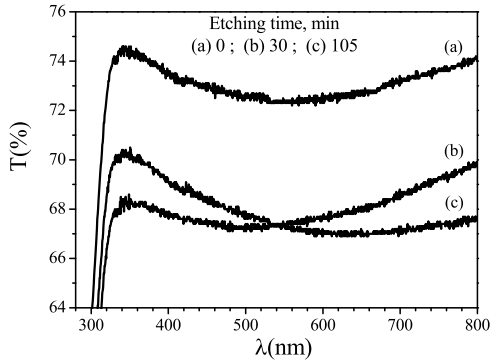

Fig. 3. The light transmittance of the film-coated TiO_2 particles after different etching times in a range of 300–800 nm light wavelength.

ture and dense film-coated TiO_2 particles were measured, as shown in Fig. 2. The corresponding TEM images of the coated TiO_2 particles were displayed in the inset. For the dense film-coated TiO_2 particles (TiO_2@SiO_2), the BET (Brunauer-Emmett-Teller) surface area and total pore volume were 13.2 m^2/g and 0.027 cm^3/g, respectively. The surface area is not large, implying that the surface was dense and smooth. However, for the sample of TiO_2@void@SiO_2, the BET surface area and total pore volume was 37.0 m^2/g and 0.102 cm^3/g, respectively, which was much higher than the dense film-coated TiO_2 particles, indicating that the coating film was porous after etching by NaOH solution.

To investigate the effect of etching time on the light reflectivity of the film-coated TiO_2 particles, the TiO_2 particle slurry at different etching times was mixed with glycerol to prepare a stable TiO_2 suspension with concentration of 0.05 g/L. The light transmittance of the TiO_2 particle suspension at different etching times was measured and is shown in Fig. 3. Fig. 3 shows that the light transmittance of the coated TiO_2 particle suspension decreased significantly, that is, the reflection and scattering ability of coated TiO_2 particles in suspension increased after etching. The film-coated TiO_2 particles with yolk-shell structures have stronger light reflection/scattering ability, i.e., higher hiding power, compared with dense film-coated TiO_2 particles.

According to the literature [17,18], the yolk-shell coated TiO_2 particles have poor weather durability. An inert dense inorganic-coated film can capture and annihilate the electrons and holes generated by TiO_2 particles under UV irradiation and suppress the photocatalytic reaction of the surrounding organic matter caused by the electrons and holes, increasing the weather durability of TiO_2 particles [5]. To increase the weather durability of the coated TiO_2 particles with the yolk-shell structure of silica, a dense film was coated on the TiO_2 particle surface. For a high stability of the coated films in the alkaline environment during silica etching process, MgO was chosen as the coating material. The silica yolk-shell structure for the TiO_2 particles coated with MgO film (TiO_2@MgO@void@SiO_2) was produced through surface-protected etching with PVP, as shown in Fig. 4. A dense MgO film was coated on the TiO_2 particle surface, and a silica yolk-shell structure was coated on the outside of the MgO film. For the current common product Si3 + Al2 in industry, the TiO_2 particles are coated with a dense SiO_2 film first, and then coated with a dense Al_2O_3 film. The coating amounts for silica content (SiO_2/TiO_2) and alumina content (Al_2O_3/TiO_2) are 3% and 2%, respectively. The Si3 + Al2-coated TiO_2 particles were prepared using the same process in industry as a reference sample.

3.2. Weather durability of the yolk-shell coated TiO_2 particles

The weather durability of the film-coated TiO_2 particles was determined by measuring the degradation rate constant of rhodamine-B. A set amount of the film-coated TiO_2 particles was dispersed in rhodamine-B solution, and the concentration of rhodamine-B was measured after UV irradiation. The curves of the apparent degradation of rhodamine-B vs. time for the film-coated TiO_2 particles with a different structure were measured and shown in Fig. 5. It shows that the apparent degradation rate constant, K_{app}, of uncoated TiO_2 particles, Si3 + Al_2-coated TiO_2 particles, and the silica dense film-coated TiO_2 particles with 20 wt% coating was 6.7, 1.8 and 0.5, respectively. The degradation rate of the rhodamine-B by the film-coated TiO_2 particles decreased, and the weather durability increased after the film coating. However, the apparent degradation rate constant of TiO_2@void@SiO_2 was 13.2, even higher than the apparent degradation rate constant of the uncoated TiO_2 particles, which have a consistency with the photocatalytic activity of yolk-shell coated TiO_2 particles reported in literature [17,18]. For a different structure of the film-coated TiO_2 particles in rhodamine-B solution at the same initial concentration, the concentration of rhodamine-B solution was measured after a sufficient adsorption in the dark for 30 min, as shown in Table 1. The concentration of

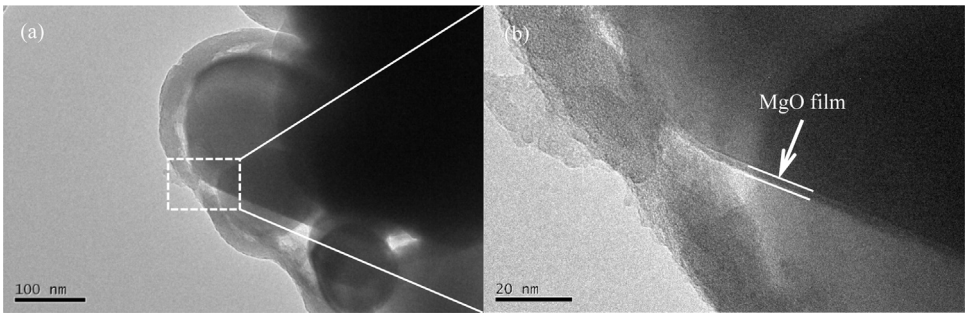

Fig. 4. The TEM image of MgO film-coated TiO_2 particles with yolk-shell structure of silica (a) and MgO film on the TiO_2 particle surface (b).

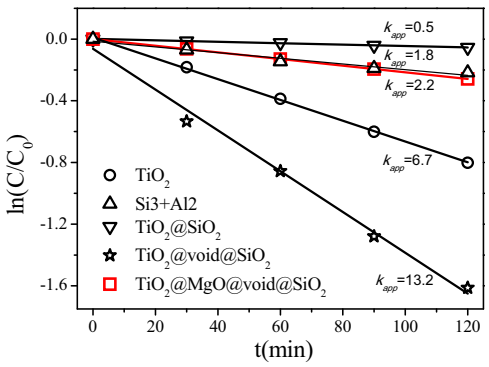

Fig. 5. Degradation of rhodamine-B by different film-coated TiO_2 particles.

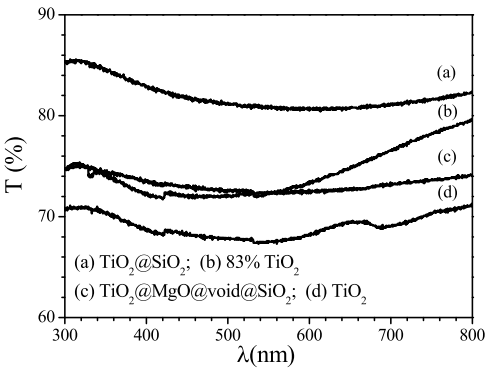

Fig. 6. The light transmittance of the TiO_2 particle suspension with a different coating film structure in the range of 300–800 nm wavelength.

Table 1
The concentration of rhodamine-B in TiO_2 suspension after dark adsorption for 30 min.

Sample	TiO_2	TiO_2@SiO_2	TiO_2@void@SiO_2
C (mg/L)	3.30	3.24	2.66

rhodamine-B in uncoated TiO_2 particles and dense film-coated TiO_2 particles (TiO_2@SiO_2) suspension was approximately 3.30 mg/L, while the concentration of rhodamine-B in the TiO_2@void@SiO_2 suspension was only 2.66 mg/L. The yolk-shell structure can adsorb more rhodamine-B compared with the dense film, leading to a high initial degradation rate of the rhodamine-B by the TiO_2 particles under UV irradiation. It indicated that the film-coated TiO_2 particles with the yolk-shell structure had poor weather durability because the coated film with the yolk-shell structure had a larger specific surface area than the dense film, and the rich internal and external surface was conducive to the contact of TiO_2 particles and rhodamine-B.

The apparent degradation rate constant of rhodamine-B for the improved yolk-shell structure coated TiO_2 particles (TiO_2@MgO@void@SiO_2) K_{app} was 2.2, indicating a significantly higher weather durability than the coated TiO_2 particles with the yolk-shell structure of silica, which was equivalent to the Si3 + Al2. The weather durability increased when the surface of TiO_2 particles was coated with a dense MgO film. The MgO film prevents the generation of radicals, decreasing the degradation rate of the rhodamine-B.

3.3. Hiding power of the yolk-shell coated TiO_2 particles

According to the measuring method of the hiding power for TiO_2 particles, the film-coated TiO_2 particles were mixed with alkyd resin to prepare the paint layers, and the hiding powers of the film-coated TiO_2 particles were determined by measuring the reflectivity of the paint layers, as shown in Table 2. The hiding power of the TiO_2@void@SiO_2 and TiO_2@MgO@void@SiO_2 having yolk-shell structure were both 90.6, while the hiding power of the TiO_2@SiO_2 with dense film-coated was only 87.7, although they have the same amount of coating. The Si3 + Al2-coated TiO_2 particles have the hiding power of 89.5 and their coating amount is 5%. Because the Si3 + Al2 sample has a lower equivalent refractive index of the film than TiO_2@SiO_2 samples, so the Si3 + Al2 sample has larger refractive index difference between core TiO_2 particles and the surroundings and has higher hiding power. Because the void structure in the TiO_2@void@SiO_2 sample results in large refractive index difference between core TiO_2 particles and the surroundings, the yolk-shell structure coated TiO_2 particles have high hiding power.

To further investigate the effects of film structure on the light reflectivity, the stable suspension of the dense film-coated TiO_2 particles and the coated TiO_2 particles with the yolk-shell structure (TiO_2@MgO@void@SiO_2) was prepared with TiO_2 particle content of 0.05 g/L according to the operation procedure in Section 2.4. The coating amount of above samples was 20 wt%, i.e., TiO_2 content for both was 83 wt%. The light transmittance of the suspension in the range of 300–800 nm wavelength was measured. For comparison, the suspensions of uncoated TiO_2 particles with concentrations of 0.05 g/L and 0.0415 g/L were prepared, and the corresponding samples were marked as TiO_2 and 83% TiO_2. The light transmittance of the above four samples was measured and is shown in Fig. 6. The suspension of uncoated TiO_2 particles had the lowest light transmittance, corresponding to the highest hiding power of the TiO_2 particles, but they cannot practically be applied because of their poor weather durability. The other three samples had the same content of TiO_2, and the dense film-coated TiO_2 particle sample had the highest light transmittance, corresponding to the lowest hiding power of the TiO_2 particles because the refractive index difference between the core TiO_2 particles and the dense silica films decreased, reducing the light reflectivity of the suspension. Fig. 6 shows that the light transmittance of the sample TiO_2@MgO@void@SiO_2 was similar to the light transmittance of the sample 83% TiO_2 because TiO_2@MgO@void@SiO_2 had a hollow shell structure, the surroundings of the TiO_2 particles were voids. The water and glycerol diffused to the voids of the porous yolk-shell structure, making TiO_2@MgO@void@SiO_2 and uncoated TiO_2 particles have the similar surroundings in the refractive index, so the suspensions have a similar light transmittance. Therefore, for the same amount of TiO_2, the different film structure coated on TiO_2 particles resulted in different light reflectivity of the TiO_2 particles. The yolk-shell structure for the dense MgO film-coated TiO_2 particles (TiO_2@MgO@void@SiO_2) gave an excellent hiding power for the TiO_2 particles.

3.4. Advantages of the improved yolk-shell coated TiO_2 particles

For uncoated TiO_2 particles (i.e., pure TiO_2), the MgO film-coated TiO_2 particles with the silica yolk-shell structure

Table 2
Hiding power of the coated TiO_2 particles with different film structure.

Sample	TiO_2@void@SiO_2	TiO_2@MgO@void@SiO_2	TiO_2@SiO_2	Si3 + Al2
Hiding power (%)	90.6 ± 0.3	90.6 ± 0.3	87.7 ± 0.3	89.5 ± 0.2

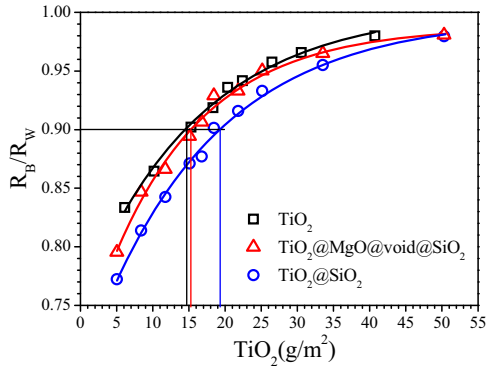

Fig. 7. R_B/R_W change with the amount of TiO_2 per unit area for different TiO_2 particles.

(TiO_2@MgO@void@SiO_2) and TiO_2 particles coated with a dense SiO_2 film (20 wt%, TiO_2@SiO_2), R_B/R_W change with the amount of TiO_2 per unit area was measured and is shown in Fig. 7. When the amount of TiO_2 is less than approximately 50 g/m^2, the amount of TiO_2 has a significant influence on R_B/R_W. The ratios R_B/R_W are, in descending order, pure $TiO_2 \approx TiO_2$@MgO@void@$SiO_2 > TiO_2$@SiO_2. It shows that the hiding power of the improved yolk-shell coated TiO_2 particles is about the same as that of the uncoated TiO_2 particles, and much higher than that of the dense coated TiO_2 particles.

Setting the ratio $R_B/R_W = 0.90$, the amount of TiO_2 per unit area of 14.8, 15.2 and 19.3 g/m^2 were required for pure TiO_2, TiO_2@MgO@void@SiO_2 and TiO_2@SiO_2, respectively, which are shown in Fig. 7. For the same R_B/R_W, the pure TiO_2 dosage using TiO_2@MgO@void@SiO_2 was reduced by 21.2% compared with using the dense SiO_2-coated TiO_2 particles (TiO_2@SiO_2). The improved yolk-shell coated TiO_2 particles have high hiding power under the premise of ensuring high weather durability, showing a great potential in applications.

4. Conclusions

TiO_2 particles coated with a yolk-shell structure of silica were prepared by PVP surface-protected etching, reaching an excellent hiding power of 90.6, significantly higher than 87.7 for the dense film-coated TiO_2 particles with the same coating amount of 20%. The voids in the yolk-shell structures increased the refractive index difference between the core TiO_2 and the surroundings, which increased the hiding power of the TiO_2 particles. However, the yolk-shell structure adsorbed rhodamine-B easily, which made the degradation rate constant K_{app} reach 13.2, reducing weather durability of the TiO_2 particles.

The TiO_2 particles were coated with a dense MgO film first and then coated with a yolk-shell structure of silica. The hiding power of the improved yolk-shell coated TiO_2 particles (TiO_2@MgO@void@SiO_2) was 90.6, and the apparent degradation rate constant K_{app} was only 2.2, which was equivalent to the common product Si3 + Al2 in industry. Compared with the same coating amount of 20% in dense film, the consumption of TiO_2 particles with the improved yolk-shell structure coated was reduced over 20% under the premise of keeping the high hiding power and weather durability properties.

Acknowledgments

The authors wish to express their appreciation for the financial support of this study by the National Natural Science Foundation of China (NSFC No. 21176134) and the National High Technology Research and Development Program (863 Program, No. 2012AA062605).

References

[1] J. Oguma, Y. Kakuma, M. Nishikawa, Y. Nosaka, Effects of silica-coating on the photoinduced hole formation and decomposition activity of titanium dioxide photocatalysts under uv irradiation, Catal. Lett. 142 (2012) 1474–1481.
[2] R. Wang, K. Hashimoto, A. Fujishima, M. Chikuni, E. Kojima, A. Kitamura, M. Shimohigoshi, T. Watanabe, Photogeneration of highly amphiphilic TiO_2 surfaces, Adv. Mater. 10 (1998) 135–138.
[3] M.L. Taylor, G.E. Morris, R.S. Smart, Influence of aluminum doping on titania pigment structural and dispersion properties, J. Colloid Interface Sci. 262 (2003) 81–88.
[4] L.F. Hakim, D.M. King, Y. Zhou, C.J. Gump, S.M. George, A.W. Weimer, Nanoparticle coating for advanced optical, mechanical and rheological properties, Adv. Funct. Mater. 17 (16) (2007) 3175–3181.
[5] B. Wei, L. Zhao, T. Wang, H. Gao, H. Wu, Y. Jin, Photo-stability of TiO_2 particles coated with several transition metal oxides and its measurement by rhodamine-B degradation, Adv. Powder Technol. 24 (2013) 708–713.
[6] Y. Liu, C. Ge, M. Ren, H. Yin, A. Wang, D. Zhang, C. Liu, J. Chen, H. Feng, H. Yao, T. Jiang, Effects of coating parameters on the morphology of SiO_2-coated TiO_2 and the pigmentary properties, Appl. Surf. Sci. 254 (2008) 2809–2819.
[7] Y. Liu, Y. Zhang, C. Ge, H. Yin, A. Wang, M. Ren, H. Feng, J. Chen, T. Jiang, L. Yu, Evolution mechanism of alumina coating layer on rutile TiO_2 powders and the pigmentary properties, Appl. Surf. Sci. 255 (2009) 7427–7433.
[8] Y. Zhang, H. Yin, A. Wang, M. Ren, Z. Gu, Y. Liu, Y. Shen, L. Yu, T. Jiang, Deposition and characterization of binary Al_2O_3/SiO_2 coating layers on the surfaces of rutile TiO_2 and the pigmentary properties, Appl. Surf. Sci. 257 (2010) 1351–1360.
[9] Y. Zhang, H. Yin, A. Wang, C. Liu, L. Yu, T. Jiang, Y. Hang, Evolution of zirconia coating layer on rutile TiO_2 surface and the pigmentary property, J. Phys. Chem. Solids 71 (2010) 1458–1466.
[10] H. Gao, B. Qiao, T. Wang, D. Wang, Y. Jin, Cerium oxide coating of titanium dioxide pigment to decrease its photocatalytic activity, Ind. Eng. Chem. Res. 53 (2014) 189–197.
[11] L. Zhao, H. Gao, B. Wei, T. Wang, Y. Jin, Evaluation of photocatalytic activity of pigmentary titania, J. Chem. Ind. Eng. (China) 64 (2013) 2453–2461.
[12] W.D. Ross, Theoretical light-scattering power of TiO_2 microviods, Ind. Eng. Chem. Prod. Res. Dev. 13 (1974) 45–49.
[13] J.A. Seiner, H.L. Gerhart, Light scattering from microvoids: applications to polymer coatings, Ind. Eng. Chem. Prod. Res. Dev. 12 (1973) 98–109.
[14] Y. Liang, B. Qiao, T. Wang, H. Gao, K. Yu, Effects of porous films on the light reflectivity of pigmentary titanium dioxide particles, Appl. Surf. Sci. 387 (2016) 581–587.
[15] D. Nguyen, C. Such, B. Hawkett, Polymer–TiO_2, composite nanorattles via RAFT-mediated emulsion polymerization, J. Polym. Sci. Pol. Chem. 50 (2012) 346–352.
[16] Baker M.P., Davey T.W., Hawkett B.S., Nguyen D.N., O'Brien C.C., Such C.H., The University of Sydney, Australia, PCT Patient 2011; WO2011066608A1 pp 112.
[17] Y. Ren, M. Chen, Y. Zhang, L. Wu, Fabrication of rattle-type TiO_2/SiO_2 core/shell particles with both high photoactivity and UV-shielding property, Langmuir 26 (2010) 11391–11396.
[18] X. Wang, H. Chen, A new approach to preparation of TiO_2@void@SiO_2 rattle type core shell structure nanoparticles via titanyl oxalate complex, Colloid Surf. A 485 (2015) 25–33.
[19] A. Guerrero-Martinez, J. Perez-Juste, L.M. Liz-Marzan, Recent progress on silica coating of nanoparticles and related nanomaterials, Adv. Mater. 22 (2010) 1182–1195.
[20] K. Kamata, Y. Lu, Y.N. Xia, Synthesis and characterization of monodispersed core-shell spherical colloids with movable cores, J. Am. Chem. Soc. 125 (2003) 2384–2385.
[21] X.W.D. Lou, L.A. Archer, Z. Yang, Hollow micro-/nanostructures: synthesis and applications, Adv. Mater. 20 (2008) 3987–4019.
[22] S. Ikeda, H. Kobayashi, Y. Ikoma, T. Harada, T. Torimoto, B. Ohtani, M. Matsumura, Size-selective photocatalytic reactions by titanium(IV) oxide coated with a hollow silica shell in aqueous solutions, Phys. Chem. Chem. Phys. 9 (2007) 6319–6326.
[23] J. Lee, J.C. Park, H. Song, A nanoreactor framework of a Au@SiO_2 yolk/shell structure for catalytic reduction of p-nitrophenol, Adv. Mater. 20 (2008) 1523–1528.
[24] Q. Zhang, T. Zhang, J. Ge, Y. Yin, Permeable silica shell through surface-protected etching, Nano Lett. 8 (2008) 2867–2871.
[25] Q. Zhang, J. Ge, J. Goebl, Y. Hu, Z. Lu, Y. Yin, Rattle-type silica colloidal particles prepared by a surface-protected etching process, Nano Res. 2 (2009) 583–591.
[26] A. Fujishima, X. Zhang, D.A. Tryk, TiO_2 photocatalysis and related surface phenomena, Surf. Sci. Rep. 63 (2008) 515–582.
[27] D.S. Bhatkhande, V.G. Pangarkar, A. Beenackers, Photocatalytic degradation for environmental applications – a review, J. Chem. Technol. Biotechnol. 77 (2002) 102–116.
[28] A.L. Linsebigler, G.Q. Lu, J.T. Yates, Photocatalysis on TiO_2 surfaces – principles, mechanisms, and selected results, Chem. Rev. 95 (1995) 735–758.
[29] M.A. Fox, M.T. Dulay, Heterogeneous photocatalysis, Chem. Rev. 93 (1993) 341–357.

[30] J.M. Herrmann, Heterogeneous photocatalysis: fundamentals and applications to the removal of various types of aqueous pollutants, Catal. Today 53 (1999) 115–129.
[31] Y. Li, S. Sun, M. Ma, Y. Ouyang, W. Yan, Kinetic study and model of the photocatalytic degradation of rhodamine B (RhB) by a TiO_2-coated activated carbon catalyst: effects of initial RhB content, light intensity and TiO_2 content in the catalyst, Chem. Eng. J. 142 (2008) 147–155.
[32] Comparison of contrast ratio (hiding power) of white pigments. China (GB/T 5211.17), (1988).